OPTIMIZATION OF A RADAR IN ITS ENVIRONMENT BY GEESE* TECHNIQUES

Eugene L. Berger and Robert M. Taylor
Advance Systems Engineering
Defense Systems Department
General Electric Company
Syracuse, New York

SECTION I

Summary

One of the most complex problems in optimization of ground radars is the evaluation of the ground clutter and how it influences the operation of the radar. A fundamental limitation of ground radars is that the radar is unable to distinguish stationary targets in the presence of large amounts of random scatterers. The capability of a phase comparison radar to pick the stationary targets out of random scatterers has been evaluated on GEESE under a contract for Frankford Arsenal in Philadelphia, Pa. A model of Frankford Arsenal's radar was built on the GEESE analog computer facility and tested in single and multiple target situations in an environment consisting of random scatterers (clutter). This was accomplished by simulating mathematical characteristics of ground clutter and applying this as an input to the simulated model. This report deals with the GEESE application, an optimization of a general radar block diagram. The optimization is carried out under an arbitrary set of boundary conditions for the overall system.

A Discussion of GEESE

General Electric developed analog simulation techniques for evaluating entire electronic systems to meet the need for a faster, less expensive means for evaluating, analyzing and developing weapon systems.

In considering a system evaluation, there are four basic facts to remember:

1. Any signal can be generated and controlled easily.

2. All signals and waveforms can be recorded - this includes transients as well as steady state signals.

3. Feasibility studies can be undertaken on a simulated basis prior to development of system hardware.

4. No equipment need be procured for this preliminary investigation.

Thus GEESE permits the electronic system engineer to predict and optimize system performance.

GEESE techniques were pioneered at General Electric on the interference program associated with the development of the radio-command guidance system for the Air Force Atlas. A facility exists at General Electric's Defense Systems Department in Syracuse, New York, which is used to simulate all types of radar and communications systems and to evaluate the effects of ECM and mutual interference.

Purpose

The purpose of this study was to see if ground clutter could be simulated on the computer; and, as a check upon the simulation, the output of the clutter generator was to be compared to actual clutter. Also, the simulation of the radar was to be checked and compared to experimental data taken in the field by an actual radar which was used and designed by Frankford Arsenal, Philadelphia, Pa. Thus, if the simulation of both the clutter and the radar are correct, the results of this test should be the same as those obtained with the actual operating radar.

System Description

A radar can be analyzed by describing the transfer functions of the receiver and signal processing circuitry; thus, on the analog computer, a simulation of these transfer functions and signal processing circuitry yields the capability of analyzing all of the parameters of the radar. Second, the effects of ground clutter upon this radar can be determined by a simulation of the clutter environment. The ground clutter environment is the effect of trees, grass, bushes, and other moving objects upon the radar. In addition to these moving scatters, there are also fixed targets which are part of the ground clutter configuration. These are basically rocks, buildings, tree trunks, cliffs, ridges of earth, and other stationary man-made objects. The whole clutter environment, therefore, is quite complex in that it is composed of both random scatterers and fixed targets. It is the object of any ground radar to distinquish a particular stationary target in this complex clutter environment. The radar simulated is basically a monopulse radar. This means that the radar has two antennas and that simultaneous lobing occurs such that the phase of the target returns is the measure of the location of a given stationary target in azimuth, and the occurrence of the pulse is a measure of the range of the particular target. In this monopulse radar, there are two channels, a sum and a difference channel. The sum channel is the sum of all the instantaneous voltages arriving at the two antennas while the difference channel is the difference of the instantaneous signals arriving at the antennas. These signals are then bandpassed in an IF strip and video detected. The

* General Electric Electronic Systems Evaluator

video signal is integrated and processed by boxcarring. These boxcarred signals are then subtracted and the final presentation is this subtraction of boxcars. When a given fixed target is on boresight and there is no clutter, then a maximum will occur in the sum channel when a minimum occurs in the difference channel. If these two signals are then video detected and boxcarred, the sum channel boxcars will then be a maximum while the difference channel boxcars will be a minimum. The subtraction of these two boxcars will yield positive boxcars. If there is no target, only random scatters, then the sum and difference channels will have independent random noise signals and the boxcar outputs of each channel will be both positive and negative. The subtraction of these two signals will give a boxcar output which varies around zero both positive and negative; thus, in this system, a positive boxcar output is an indication of a target.

Area of Investigation

The radar was investigated in fundamental form in different clutter environments. A range of target to clutter power ratios was investigated by varying the amount of clutter input. The clutter was characterized by wind speed and the particular center frequency of the radar. The radar was also investigated in a fundamental form without any clutter by supplying only target information to the radar. The target was then moved in azimuth across the antenna pattern of the radar. This determined the sum and difference patterns of the respective channels of the radar. The radar again was investigated in its fundamental form when two targets were the only input to the radar. By varying the two targets in azimuth across the antenna beamwidth, the interaction in either the sum or difference channel could be noted.

SECTION II

Simulation

GEESE Simulation

The analog computer simulation of this radar is a scale model of the given system and not an analog. In all systems simulated on GEESE, only a scaling of frequencies occurs with gain relationships, voltages, and currents remaining in the same order of magnitude. More important, certain non-linearities are taken into account. Waveforms observed at the terminals of system elements are identical to those in the actual system except for time scaling. On the whole, the simulation is highly idealized compared to the actual system. The amplifiers and integrators are linear over their entire range, and system elements such as a linear detector are extremely linear. The input frequencies to the analog computer can be made to have the same order of stability as those experienced in the actual system. Noise inputs are purely Gaussian in amplitude and white in power density. The signal levels put into the analog computer were held constant without the action of an AGC loop, and the input frequencies were held constant without an AFC loop.

The Simulation of Ground Clutter

Actual clutter is characterized by power frequency spectrum and a correlation function. The clutter generator simulates these characteristics as frequencies scaled compatibly with the radar parameters under consideration. The power frequency spectrum and the correlation function simulated were determined from a study of actual clutter. In a situation involving random scatterers (clutter) and a single stationary target, the composite return has a Rayleigh distribution. As the target level increases, the probability density function of the signal power approaches a Gaussian distribution. The mean of this Gaussian probability density function is the signal power of the target. Appendix 1 presents a mathematical analysis of clutter.[1]

The clutter supplied to the simulated radar comes from a clutter generator which implements this mathematical model of ground clutter. This generator implements and incorporates some of the features particular to the radar in this study and includes the flexibility required to simulate a wide variety of environmental conditions. The clutter generator, in general, provides two basic components of clutter. The first is random scatterers, which consist of the returns from leaves and grass in various wind speeds up to gale winds. The second main component of clutter is stationary targets. These targets are representative of dense woods, rocks, boulders, and other ground environments which are stationary. The clutter generator can position these stationary targets in range and in return power. Also, the clutter generator can position the stationary targets in azimuth. Another capability of the clutter generator is to simulate amplitude and frequency of range jitter. This can correspond to frequency instability in the transmitter or to the motion of a given fixed target.

The block diagram shown in Figure 1 represents the signal processing which is carried on in the clutter generator. Each channel receives equivalent power returns from a collection of random scatters, two parasitic targets varying in range, and one fixed target. The random scatters have the characteristics of the purely theoretical random scatters in that the probability distribution of the amplitudes is a Rayleigh distribution and correlation function is equivalent to that observed in experimental data. Also, the amplitude frequency spectrum of the random scatterers is based upon the experimental findings of clutter returns at different wind speeds for various RF center frequencies.

In the block diagram, four independent Gaussian noise sources are used to modulate two carrier components in phase and quadrature. These components are added and then supplied to both the sum and difference channels. The output of the sum amplifier in the block diagram is then Rayleigh distributed in amplitude and has a power frequency spectrum corresponding to a particular wave length of the radar and the wind speed of the environment. When a main target is introduced into the summing amplifier in the block diagram, the output is now Gaussian distributed in amplitude having a mean about the average amplitude return from the steady target. By varying the main target in amplitude and phase, so as to simulate frequency instability or motion of the target, the output of the summing amplifier in the block diagram changes from the Rayleigh

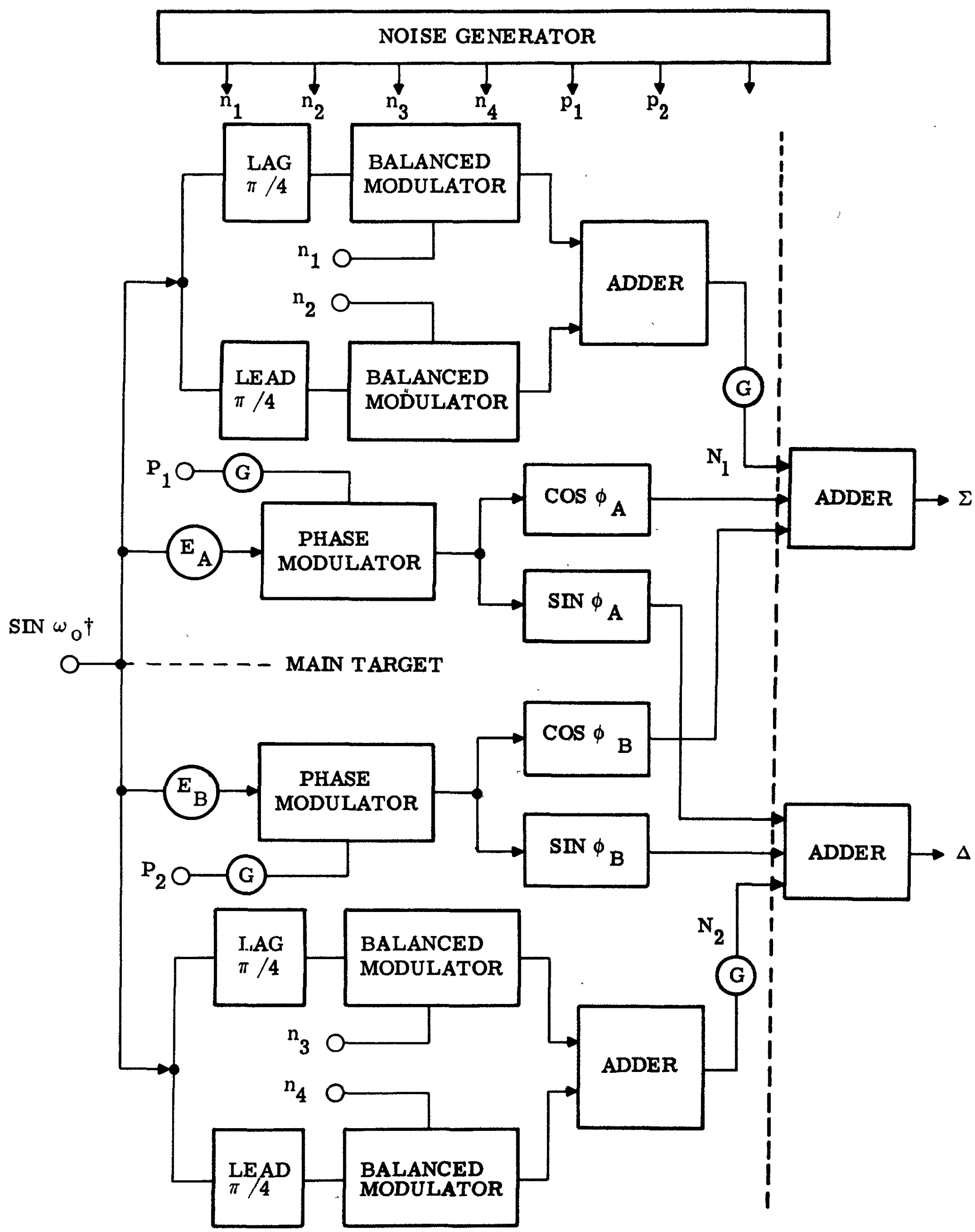

Figure 1. Block Diagram, Signal Processing of a 400-CPS Carrier

distribution in amplitude to a particular Gaussian distribution in amplitude, therefore, describing the theoretical probability distributions for signal plus noise where the signal is also varying in amplitude and phase. The parasitic targets in the block diagram are introduced through the phase modulator and resolving potentiometers which respectively jitter the targets in range and describe their positions in azimuth.

This whole scheme is based on the instantaneous sum and difference signals appearing in a monopulse radar. The sum phasor is multiplied by the cosine of the respective electrical angles off boresight; and, in the difference channel, the instantaneous phasor is multiplied by the sine of the respective electrical angles off boresight. These equations follow.

$$e_{sum} = \mathrm{Re}\left\{ 2 \left[\tilde{E}_A \cos \phi_A + \tilde{E}_B \cos \phi_B \right] e^{jw_o t} \right\}$$

$$e_{difference} = \mathrm{Re}\left\{ 2 \left[\tilde{E}_A \sin \phi_A + \tilde{E}_B \sin \phi_B \right] e^{jw_o t} \right\}$$

The noise generator in the block diagram is essentially a tape unit plus two low-pass filters which give the amplitude versus frequency spectrum of the noise and the correlation function of ground clutter. This is illustrated in Figure 2 which shows how the frequency spectrum is set and the correlation function is obtained by two low-pass filters. Appendix 2 describes how the correlation function is achieved by two low-pass filters. Knowing the frequency spectrum coming out of the tape unit and the power density of this noise, the output power of the two low-pass filters can be calculated by the following equation which has been derived in Appendix 3.

$$\therefore \overline{x_2^{\,2}} = \frac{a^2 A^2}{w_1^{\,2} 2} \left[\frac{1}{1 + (w_o/w_1)^2} + \frac{w_1}{w_o} \mathrm{Tan}^{-1} \frac{w_o}{w_1} \right] \overline{x_o^{\,2}}$$

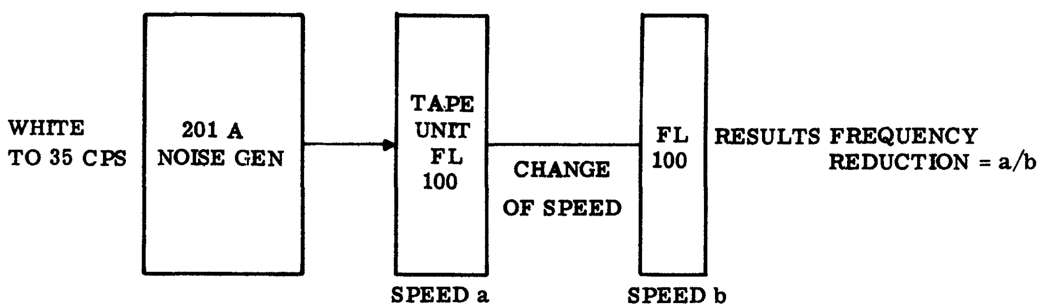

if $a = 60$ in. /sec $\qquad \frac{a}{b} = 8$

$b = 7\text{-}1/2$ in. /sec

$\therefore$ The new spectrum is white to $\frac{35}{8} = 4.37$ cps

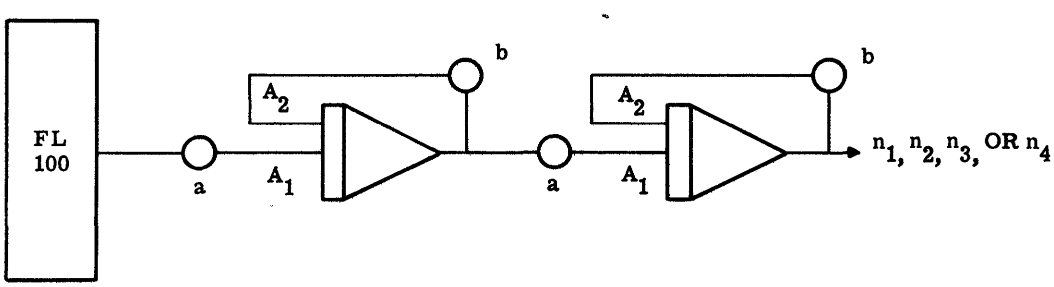

Various values of a and b are determined by wind speed and the rms output level.

Figure 2. Sequence of Operation

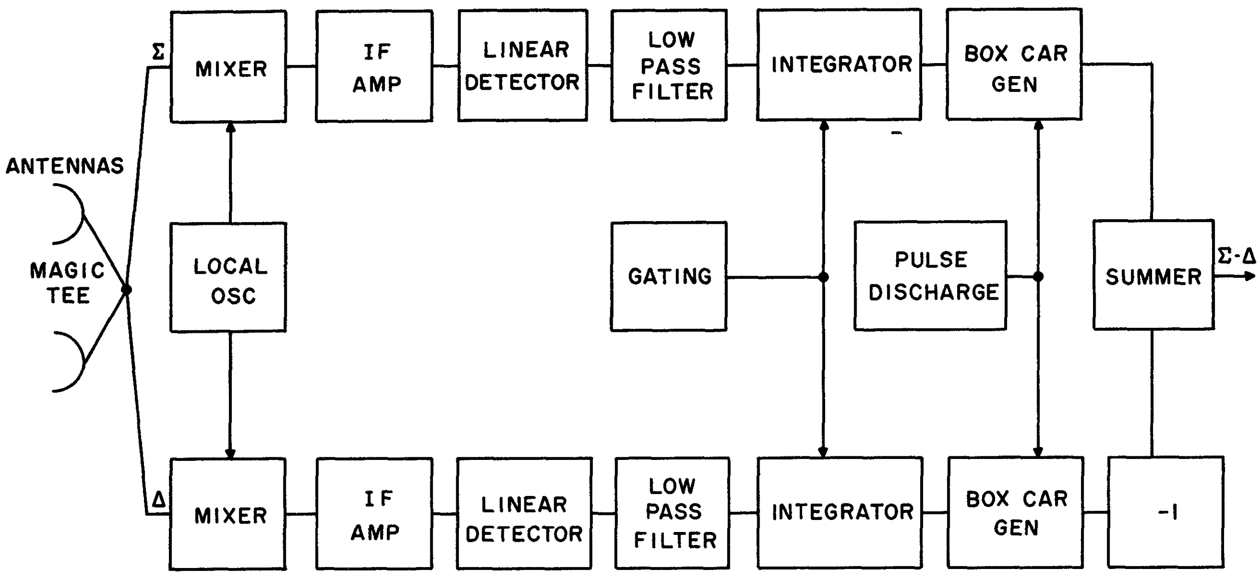

Figure 3. Radar Receiver Block Diagram

<u>General Description of the Simulated Radar</u>

The block diagram in Figure 3 is that of the radar receiver simulated on the GEESE analog computer. The block diagram consists of two antennas, a magic T, a first detector, a second detector, and a third detector. After the third detector, there is a boxcar generating circuit and a subtractor circuit which subtracts the sum and difference boxcars.

The magic T is simulated in the clutter generator so that the sum and difference of the antenna patterns are taken directly from the clutter generator. The first detector, which is a mixer converter, is simulated on the computer by a multiplier. This is shown in Figure 4. If the inputs are E_a and E_b and $E_a = A_1 \sin w_o T$ and $E_b = A_2 \sin w_1 T$, then the output is of the form

$$\frac{E_a E_b}{100} = \frac{A_1 A_2}{200} \cos (w_o - w_1) T - \frac{A_1 A_2}{200} \cos (w_o + w_1) T$$

This acts as conversion from RF to IF frequencies. The second detector is a bandpass filter which is normally referred to as an IF strip. The IF strip is centered such that only the sum frequency is passed through the IF filter. This IF filter also has the characteristics of the original radar in that it has a bandwidth equivalent to the IF of the experimental radar, and it also has a center frequency equivalent to the center of the experimental radar. The transfer function is identical to that of the experimental radar in that the simulated IF is a staggered tuned triplet. In Figure 5 is the simulation of one of the IF amplifiers. This filter has the transfer function:

$$\frac{K_1 s}{s^2 K_2 + s K_3 + K_4}$$

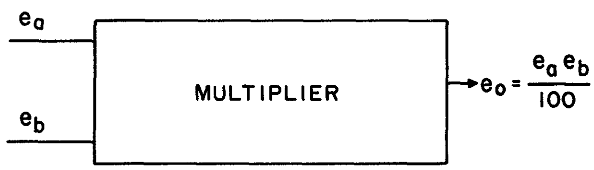

$$e_a = a_1 \quad \mathrm{SIN}\ \omega_0 t$$

$$e_b = a_2 \quad \mathrm{SIN}\ \omega_1 t$$

$$\frac{e_a e_b}{100} = \frac{a_1 a_2}{200} \mathrm{COS}\,(\omega_0 - \omega_1)\,t - \frac{a_1 a_2}{200} \mathrm{COS}\,(\omega_0 + \omega_0)\,t$$

SIMULATOR CIRCUIT

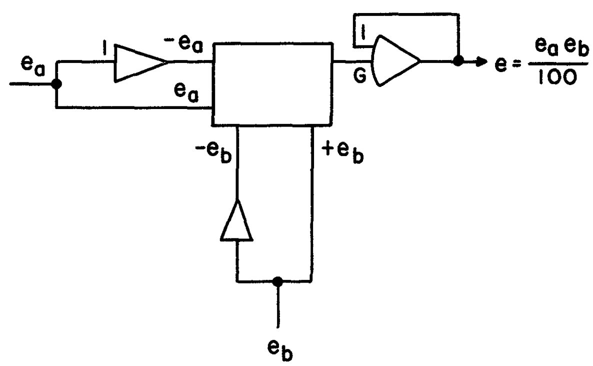

COMPUTER DIAGRAM

Figure 4. GEESE Equivalent Circuit of First Detector (Mixer)

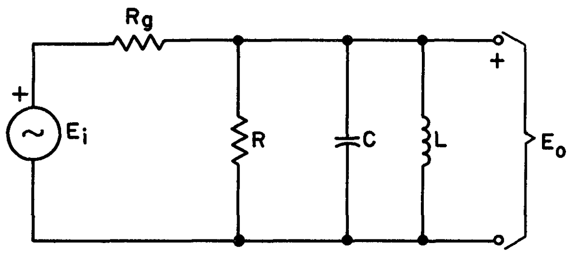

Figure 5A. Narrow Band Pass Filter

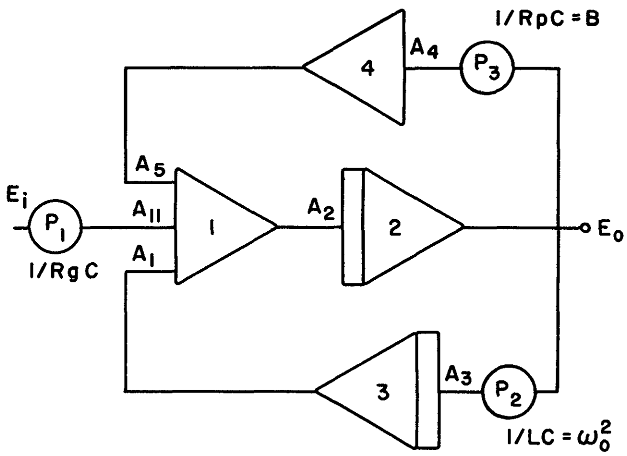

Figure 5B. GEESE Equivalent Circuit

Figure 5.

This computer simulation is the exact equivalent to a single tuned circuit. Staggered pairs and triplets can be formed by cascading several of these. In Figure 7 is the simulation of the stagger tuned triplet simulated on the computer. The first IF amplifier in this stagger tuned triplet has a relative gain of 2 and a bandwidth of 10 cycles. The second bandpass filter has a relative gain of one and has a bandwidth of 20 cycles per second. The third is identical to the first with the exception that it is at a higher center frequency. The resultant magnitude plot of these three staggered tuned circuits is illustrated in Figure 7.

The third detector is a linear detector and a low-pass filter. The linear detector has the relationship $e_{in} k = i_b$ which is the normal characteristic curve for a perfect linear detector. The third detector is shown in Figure 6. The low-pass filter has the transfer function of:

$$H(s) = \frac{1}{s + \frac{1}{RC}} = \frac{1}{s + w_1} .$$

The bandwidth of this low-pass filter is set on the computer to that bandwidth corresponding to the third detector in the actual radar. The computer simulation of the low-pass filter can be seen in Figure 7 which is a complete GEESE model of the simulated radar.

The boxcar generator consists of an active integrator which allows integration only during the sampling period or gating period. After the gating period, the input is switched to zero so that the output of the integrator remains constant until sometime later when it is desired to discharge the integrator and to initiate the integrating again. This is all shown in Figure 7 where the circuit discharge is made through the resistances Q 09 and Q 28 at the discharge occurring time.

Table 1 gives the IF center frequencies, the RF frequency, the IF bandwidth, and other characteristics of a representative radar. Corresponding to these parameters of the radar are the computer scaled parameters. The RF center frequency was changed to 400 cycles per second since there was no information in the carrier frequency; therefore, it could be changed to any convenient carrier. The other parameters were scaled by 10^{-6} with the exception of the clutter frequen-

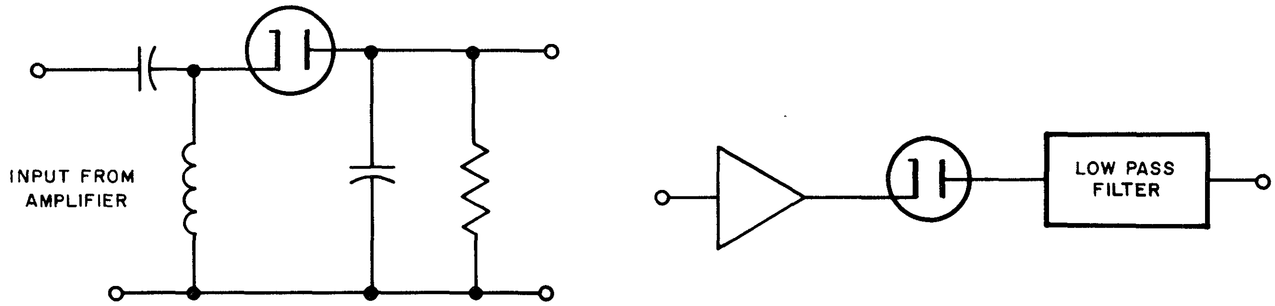

TYPICAL RADAR THIRD DETECTOR

COMPUTER EQUIVALENT CIRCUIT

Figure 6. Radar Third Detector and Equivalent Circuit

cies and the pulse repetition frequency. These two parameters were scaled to the 10^{-3} so that the computing time would not be so extremely long had it been scaled to 10^{-6}. Figure 7 includes all the filter characteristics, the boxcar characteristics, etc. The output of the two boxcar generators are subtracted from each other in an operational amplifier after the inversion of the difference channel signal. Thus, a representative radar receiver is simulated on the computer, taking into account all of the bandwidth characteristics and the transfer characteristics for each of the blocks in the radar.

Data Recording Processes

Two types of data recording are used throughout this study. The primary method is "A" scope presentations photographed for varying periods of time. The photographic process provides an accurate simulation of real time "A" scope integrations. The majority of the photographs in Section III were exposed for a period of 5 minutes. This corresponds to approximately 1200 traces, equivalent to 1/4 of a second in the real system. Twelve hundred traces are sufficient[2] to produce a stationary presentation, i.e., a reliable signal to clutter ratio.

The second method of data recording and display is eight channel oscillograph recordings. This type of data recording process enables us to examine individual traces on a continuous basis, that is, a non-integrated situation. In addition, this method enables us to monitor several points in the system to insure correct functioning of all stages of the simulated system. Data recorded in this fashion can be statistically analyzed by an examination of individual output traces in compilation of an overall statistical result for the system.

TABLE I

Radar Characteristics	Scale Factor	Computer Simulation
RF Center Frequency 35,000 mc/sec	----	400 cps
Pulse Length 0.06 μsec	10^{6}	0.06 secs
IF Bandwidth 20 mc	10^{-6}	20 cycles
IF Center Frequency 60 mc/sec	10^{-6}	60 cps
Gating Width 0.06 μsec	10^{6}	0.06 secs
Length of a Boxcar 250 milli/sec	1	250 milli/sec
Discharge Time 5 milli/sec	1	5 milli/sec
Pulse Repetition Frequency 4,000 cps	10^{-3}	4 cps
Video Bandwidth 15 mc	10^{-6}	15 cps
Clutter Frequencies X cps	10^{-3}	X 10^{-3} cps

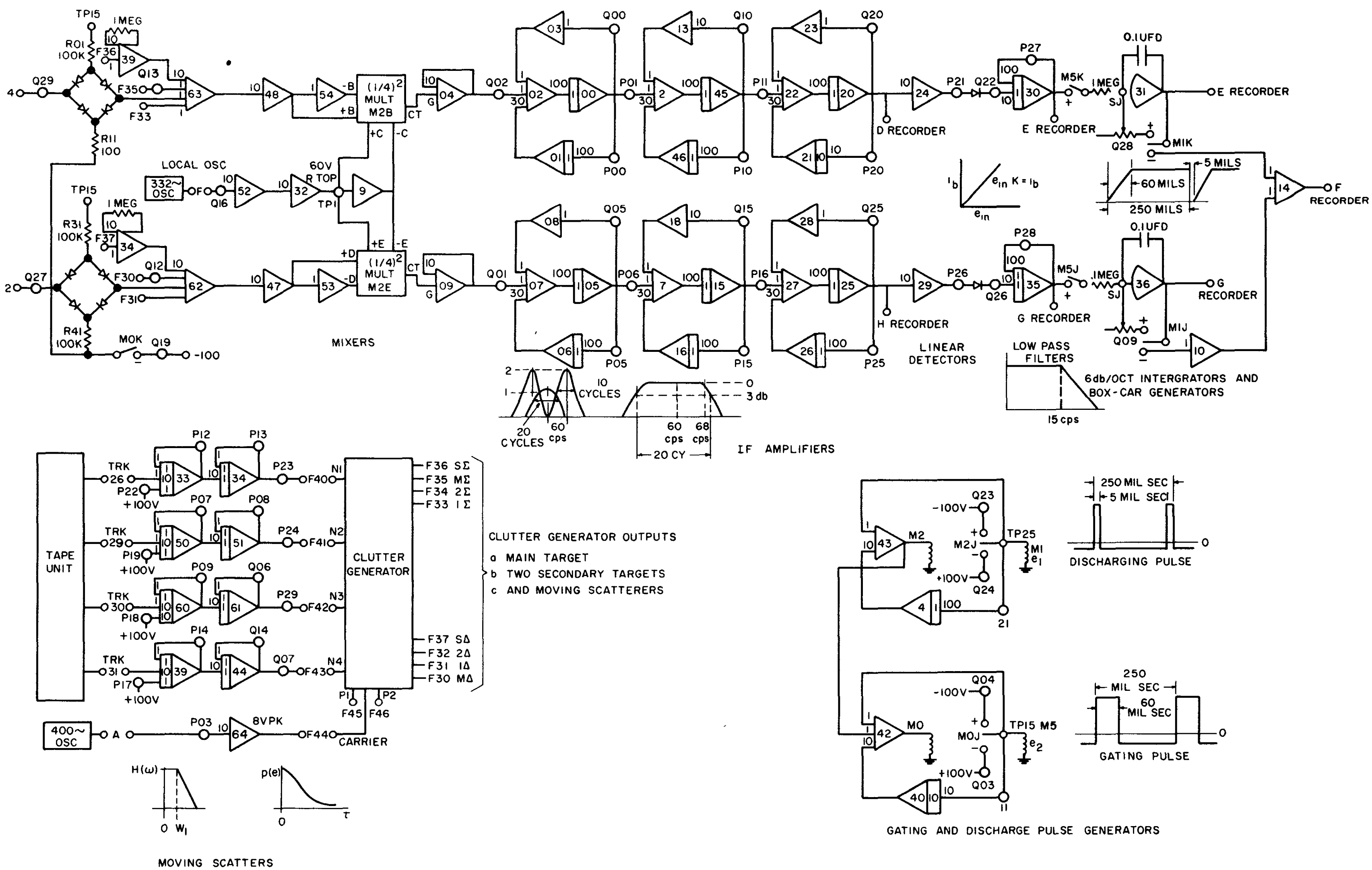

Figure 7. Complete GEESE Model of Radar Receiver

SECTION III

Results

The Investigation of Different Characteristics of the Radar

The clutter environment was applied to the simulated radar to investigate different characteristics of the radar. In the condition investigated, there was one stationary target and random scatterers. The ability of the radar to detect the stationary target was investigated for different m^2's where the m^2 is the ratio of steady power returns to random power returns. The results of this run are shown in Figure 8. In this figure, the output boxcars, which are the sum minus the difference boxcars, are shown for $m^2 = 1.32$, 2, and 4 when the main target is on boresight. The results of this show that for $m^2 = 1.32$ that the probability of detecting a target is 70 percent. The probability of detecting a target for $m^2 = 2$ is 95 percent. The probability of detecting a target for $m^2 = 4$ is 100 percent, so that on any m^2 above 4, the probability of detecting a target is always 100 percent. It can also be noted from Figure 9, which is the complete record for $m^2 = 1.32$, that the boxcars of the difference channel are that of a Rayleigh distribution in amplitude. The output of the boxcars in the sum channel are some Gaussian distribution with a mean about that of the amplitude of the target signal. This in turn verifies the output of the clutter generator to be exactly what it was designed to be. The other records in this figure are the sum and difference IF signals. These signals are essentially CW signals, but the results out of the boxcar generators are the same as they would have been had the inputs been pulsed. This is due to the fact that the boxcar generator is sampling the IF signals and integrating them only during a period of time equivalent to the time occurrence of a pulse. The only difference that can be said to exist if the inputs were pulsed is that the amplitudes of the sum and difference boxcars would be smaller due to the fact that some of the energy would have been lost due to filtering in the IF strip. An actual pulse input has been put into the computer to provide a range gated "A" scope presentation. This is shown in Figure 10.

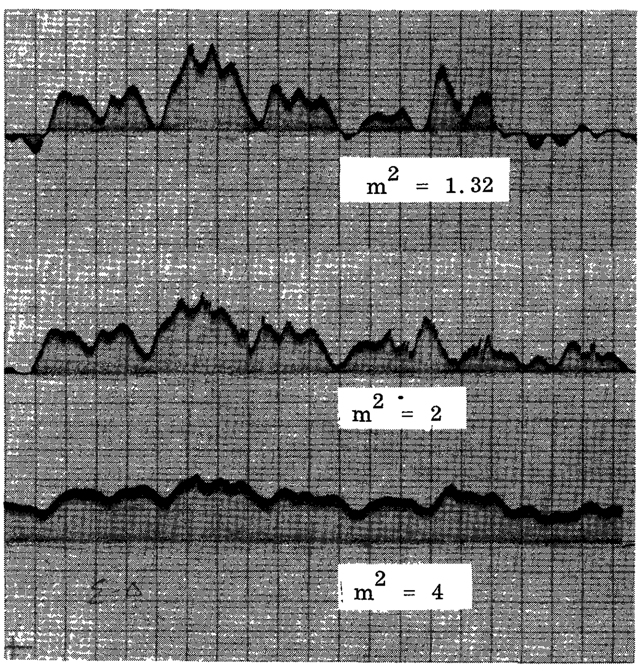

Figure 8. Single Target on Boresight in Clutter

The second investigation was to determine the system performance in the presence of two stationary targets of different sizes. Figure 11 is a series of recordings taken on the computer to determine if any interactions occur between the sum and difference channels. The strong target had twice the power of that of the small target, and the small target was jittered in phase so that the envelope of the sum and difference channels could be observed. The two targets were separated by 30 electrical degrees in azimuth. The frequency of the phase jitter on the small target was 0.3 cycle per second with a total phase deviation of 10 π radians. The different recordings are for different locations of the target and the parasitic. In all of the recordings, the main target is 30 electrical degrees to the left of the parasitic. It can be observed from the figure that the difference channel obtains its minimum when the stronger target is on boresight or its electrical position in azimuth is zero.

Figure 12 is an "A" scope presentation of two targets appearing at slightly different ranges, with the radar scans across the targets. The targets are being jittered in phase so as to simulate frequency instability or target motion.

It can be noted from these figures that the behavior of the simulated radar corresponds to that of actual radars. In fact, comparative results have shown the correspondence to be quite satisfactory for various specific situations.

At this point, optimization of the particular radar may begin. Parameters such as bandwidths, center frequencies, repetition frequency and pulse widths can be varied easily. In addition, specific antenna patterns can be investigated. This has been accomplished for a specific radar with results satisfactory to both the system engineers and the circuit designers.

As an example the video bandwidth in this report was found to be optimum at 12 cps instead of 15 cps. In addition to empirical methods of parameter optimization, analytical optimization techniques can be evaluated using these analog methods.

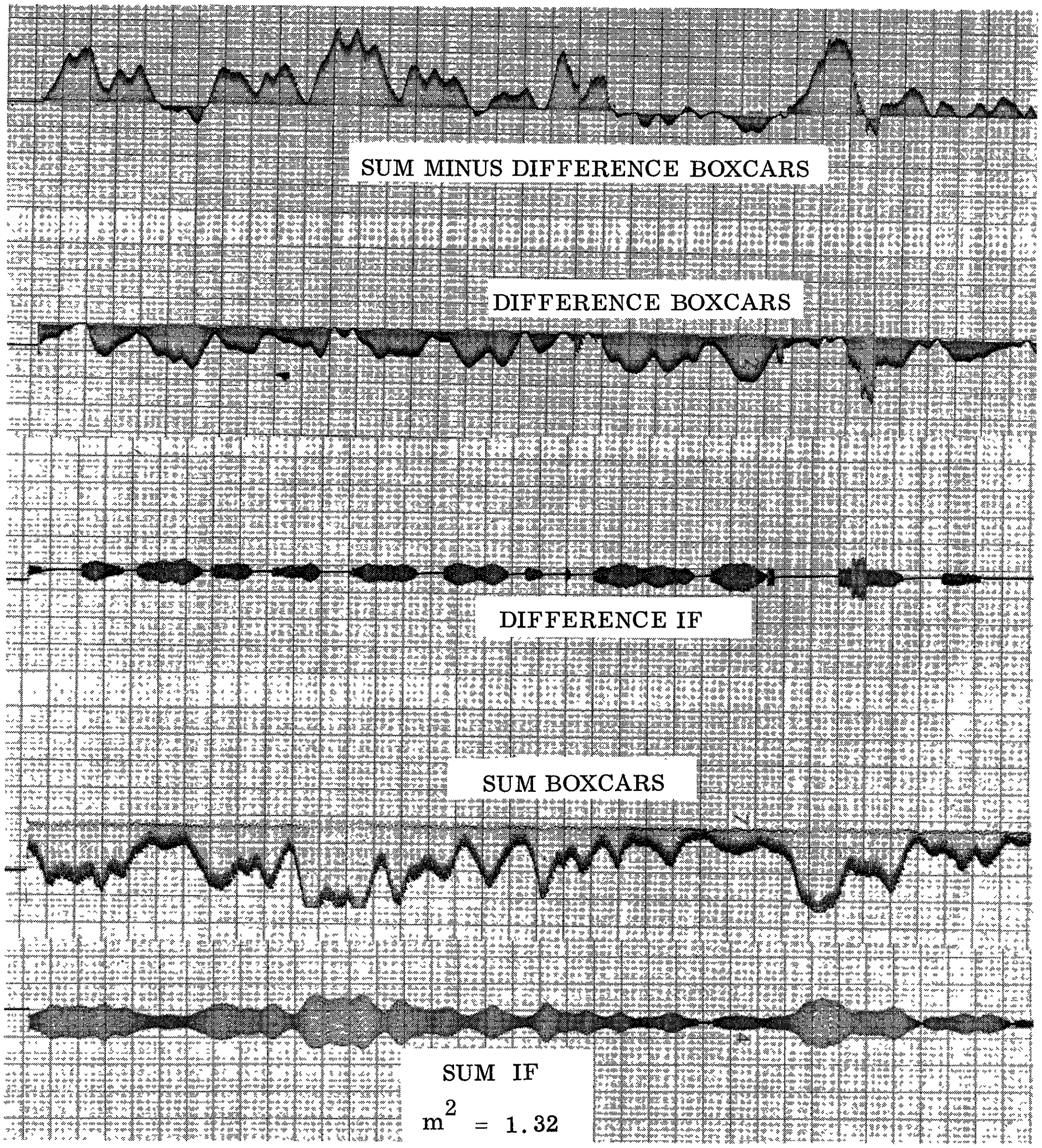

Figure 9. Single Target on Boresight in Clutter

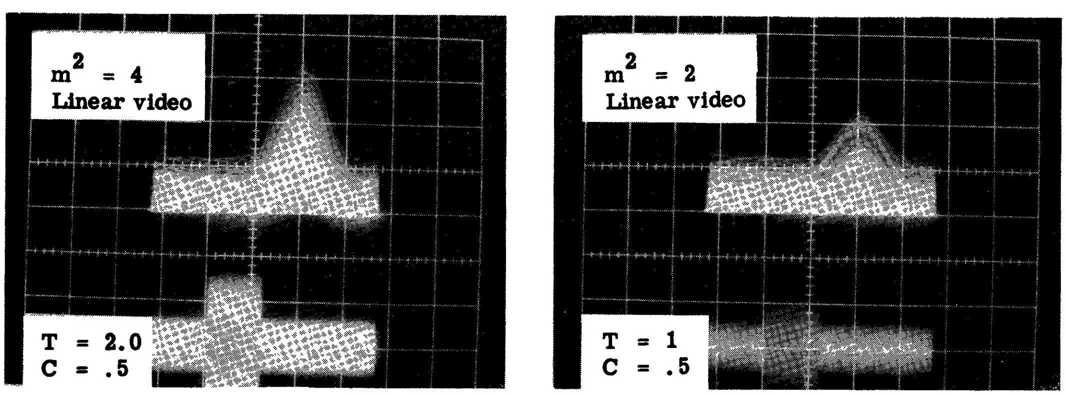

Figure 10. Single Target on Boresight in Clutter

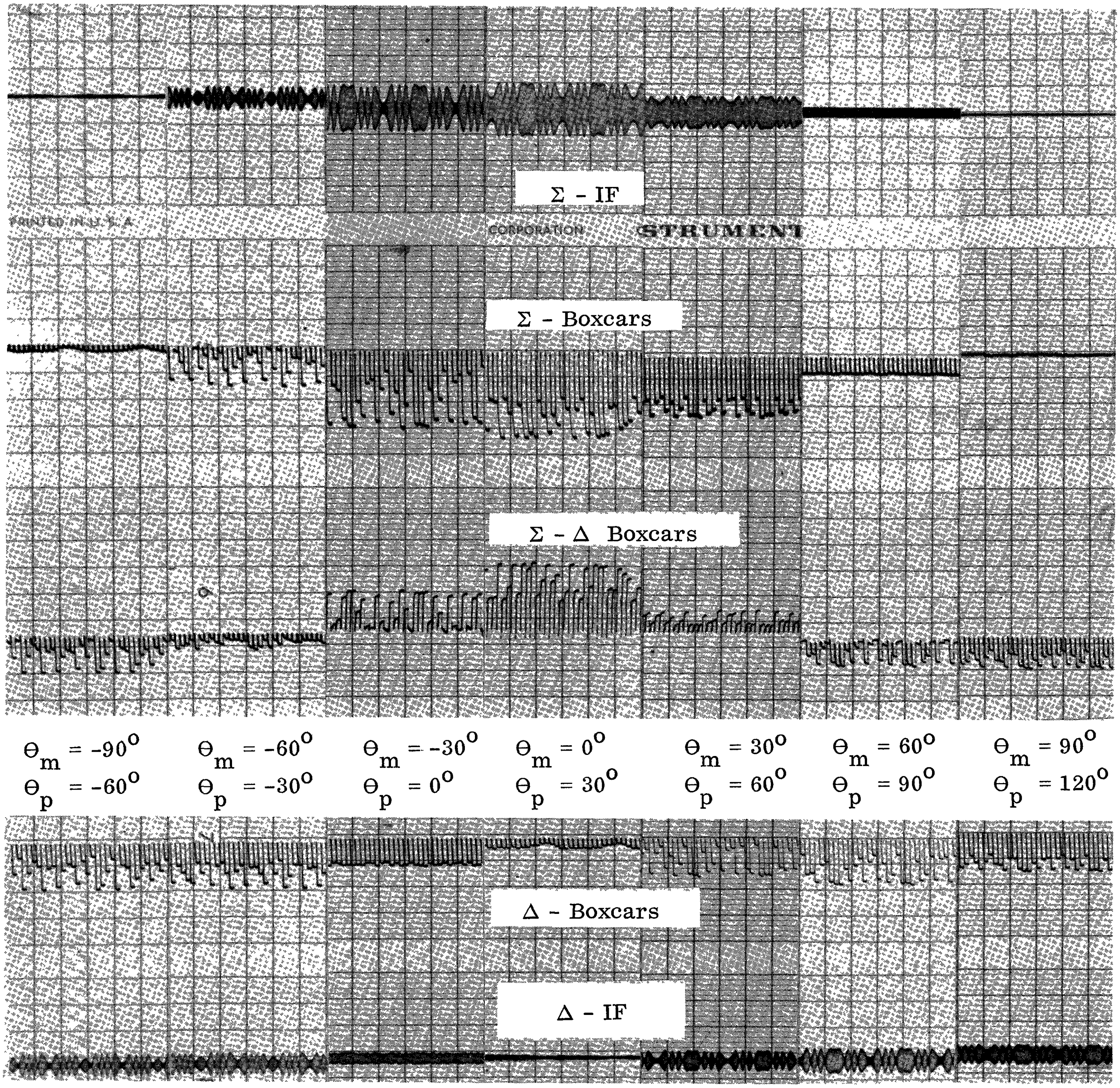

Figure 11. Two Targets Being Scanned in Azimuth

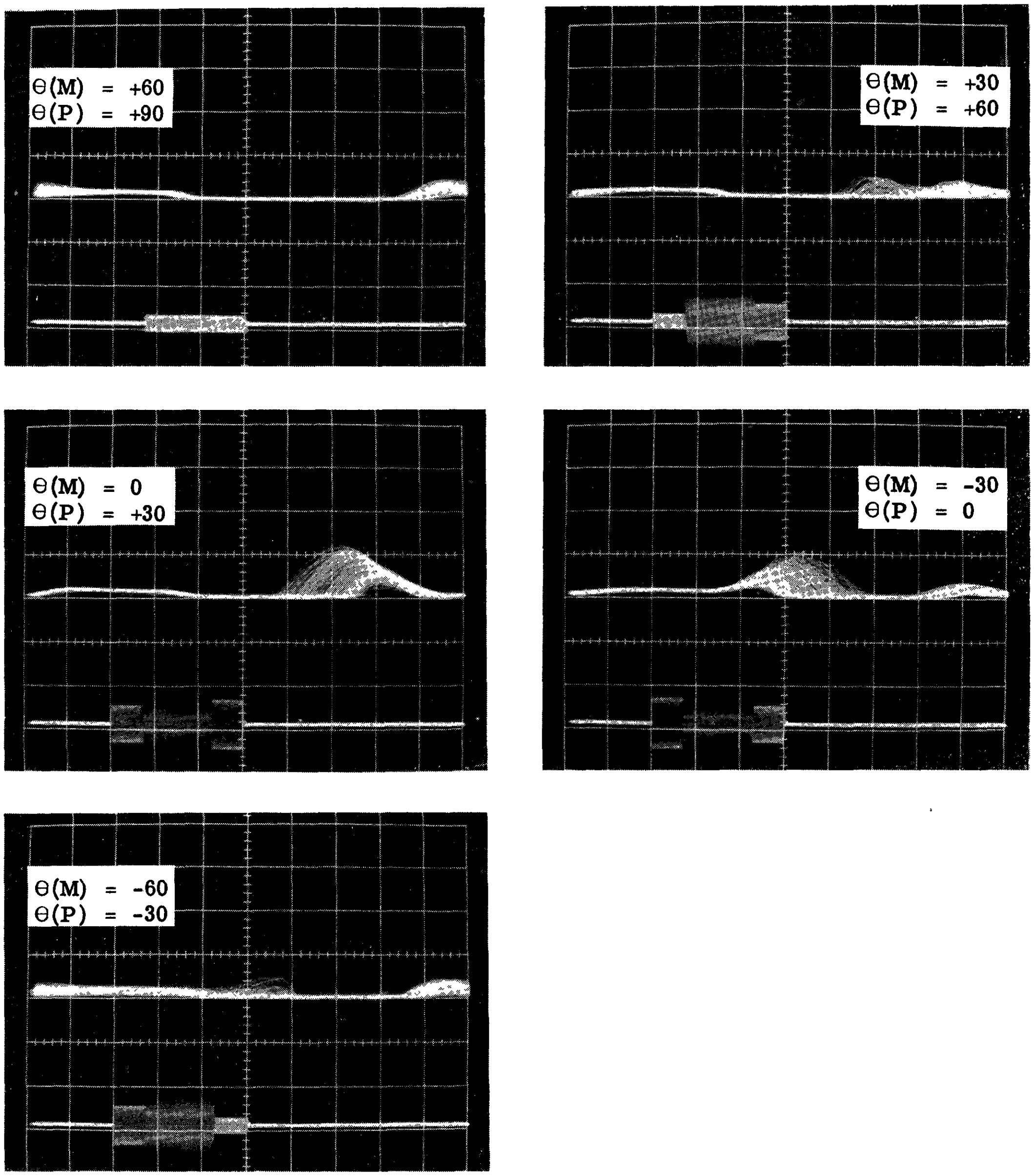

Figure 12. Two Targets Being Scanned in Azimuth, No Clutter

APPENDIX 1

Mathematical Analysis of Random Scatters

Description of Noise Envelope

Consider some of the statistical features about the envelope and phase of a random noise after passage through a narrow band filter. The frequency spread of the noise is seen to be small compared to the center frequency of w_c of the narrow band filter. If z(t) denotes the output noise record, then z(t) is equal to R(t) $\cos w_c t - \phi(t)$ with the envelope R(t). The phase angles $\phi(t)$ are allowing varying variables of time relative to oscillations of angular frequency w_c. From the previous expression z(t) can be represented as the sum of sines and cosines z(t) equal x(t) and the cosine of $w_t t - y(t) \sin \phi_c t$ where $x(t) = r(t) \cos \phi(t)$ and $y(t) = r(t) \sin \phi(t)$. This equivalent representation indicates the following relationships that $R^2 = x^2(t) - y^2(t)$ and $\operatorname{Tan} \phi(t) = \frac{y(t)}{x(t)}$.

Suppose that the joint probability density function p (x, y) is known. Then the joint probability density function p (R, ϕ) can be found from the following equation:

$$p(x, y)\, dxdy = p(R \cos \phi, R \sin \phi)\, R\, dRd\phi.$$

Since the element of area dxdy in the x, y plane corresponds to the element of area of R dRdϕ in the R, ϕ plane, let $Q(R, \phi) = R\, p(R \cos \phi, R \sin \phi)$. Then $p(x, y)\, dxdy = Q(R, \phi)\, dRd\phi$. Now the probability density function and the noise envelope Rϕ(t) alone is obtained by the sum of all phase angles and is

$$Q_1(R) = \int_0^{\beta\pi} Q(R, \phi)\, d\phi.$$

While the probability density function of the phase angle ϕ(t) alone is obtained by summing over all possible R and is

$$Q_2(\phi) = \int_0^{oo} Q(R, \phi)\, dR.$$

If x(t) and y(t) are each normally distributed about zero and mean squared values of x(t) and y(t) are equal and equal to the mean square value in c(t), also if the cross correlation function between x(t) and y(t) so that x(t) and y(t) are independent random variables, hence x(t) and y(t) can be expressed as sums of normal variables. We conclude that their joint probability density function will be two dimensional normal distribution of the form

$$p(x, Y) = p(x)\, p(y) = \frac{1e^{-\frac{x^2 + y^2}{2\sigma^2}}}{2\pi\, \sigma^2}$$

During the integration described previously, it follows a

$$Q_1(R) = \frac{Re^{-\frac{R^2}{2\sigma^2}}}{\sigma^2}$$

where $R \geq O$. This probability density function $Q_1(R)$ governs the distribution of the envelope and is known as the Rayleigh distribution. The parameter R is restricted to non-negative values. It should not be confused with the normal probability density function where the parameter may take on both positive and negative values. Solving the above integral $Q_2(\phi)$ probability density function for the phase angles $\phi(t)$ is given by $Q_2(\phi) = 1/2\,\pi$ where $0 \leq \phi \leq 2\pi$. This shows that the values of $\phi(t)$ are uniformally distributed over zero to 2π and have a rectangular distribution.[3]

The Presence of a Parasitic Target Jittering In Phase in a Clutter Environment

Let a = No. 1 parasitic target signal, rms

b = No. 2 parasitic target signal, rms

c = the phasor sum of a and b

P_o = the mean square value of the random scatters

$m^2 = C^2/P_o = C^2$ for P_o normalized to $P_o = 1$.

Assume that the probability density function of ϕ is

$$f(\phi) = \frac{1}{\pi}, \quad 0 \leq \phi \leq \pi$$

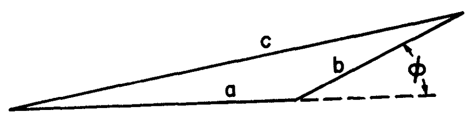

$$C^2 = a^2 + b^2 + \cos\phi = m^2$$

1. If $y = 2ab \cos \phi$, or $\phi = \cos^{-1}\left(\frac{y}{2ab}\right)$ since $f(y) = f(\phi) \left|\frac{d\phi}{dy}\right|$

2. Therefore,

$$f(y) = \frac{1}{2\pi\, ab}\left[1 - \left(\frac{y}{2ab}\right)^2\right]^{-\frac{1}{2}}$$

3. or, the probability density function of m^2 is

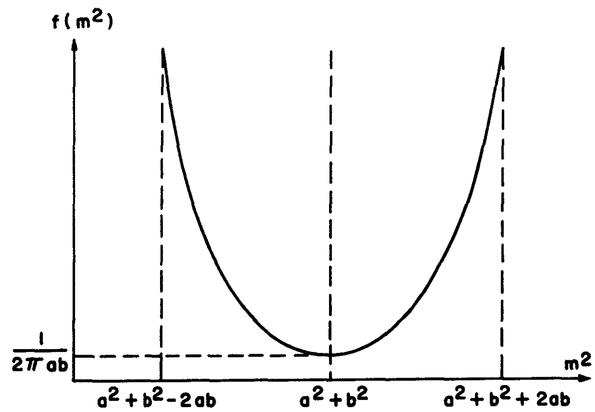

This distribution indicates the probability, $f(m^2)d(m^2)$, of obtaining a particular type of first probability distribution in power for a target consisting of random scatters and two strong targets. It can be indicated as

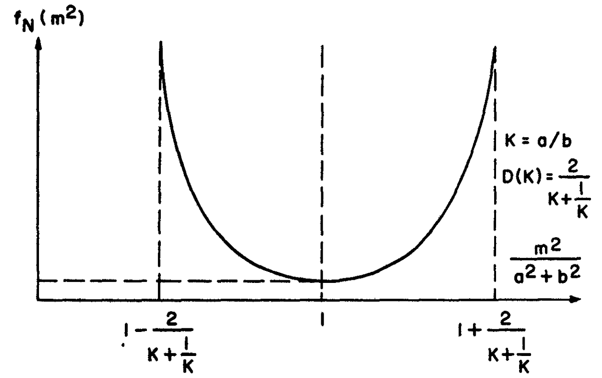

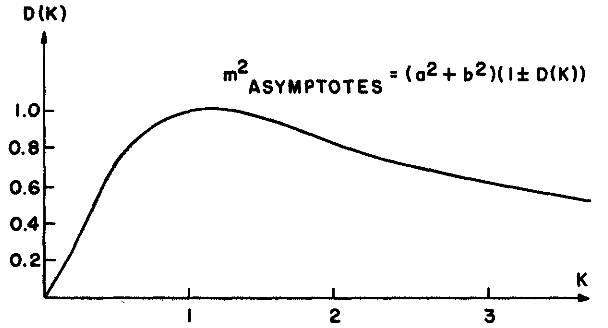

As a typical case consider that the levels of the fixed targets have been established at a_1^2 and b_1^2, and that the parasitic-1 to parasitic-2 target ratio is $K_1 = a_1/b_1$, leaving only the relative phase between a_1 and b_1 unknown. Then, we can specify with what probability we can expect to obtain an m^2 (with corresponding type of first probability distribution)

$W_1(P/\bar{P})$, which may lie only in the range,

$$a_1^2 + b_1^2 - \frac{2}{K_1 + 1/K_1} \leq m^2 \leq a_1^2 + b_1^2 + \frac{2}{K_1 + 1/K_1}.$$

Note the following:

1. The value around which m^2 may range is $a_1^2 + b_1^2$.
2. The percentage spread in m^2 is dependent on $K = a/b$; i.e., $D(K) = \frac{2}{K + \frac{1}{K}}$
3. Although the probability of having an $m^2 \leq a_1^2 + b_1^2$ always remains at 1/2, the probability with which we can predict a given type of $W_1(P/\bar{P})$ increases with K, independent of $a^2 + b^2$. This implies that under the condition that K>10, the clutter generator provides stationary statistics.

On the basis of this analysis, it is recommended that the clutter environment be characterized by:

1. $a^2 + b^2$
2. $K = a/b$

in order to use the result that

$$W_1(P)dP = (1 + m^2)\, e^{-m^2}\, e^{-P/\bar{P}\,(1 + m^2)}\, J_0\left(2im \sqrt{1 + m^2} \sqrt{\frac{P}{\bar{P}}}\right) \frac{dP}{\bar{P}}$$

First probability distribution in power for a target consisting of random scatters plus a fixed target, for several values of $m^2 = S^2/P_o$.

S^2 = steady power

P_o = random power

Ref: Vol. 13 Radiation Laboratory Series

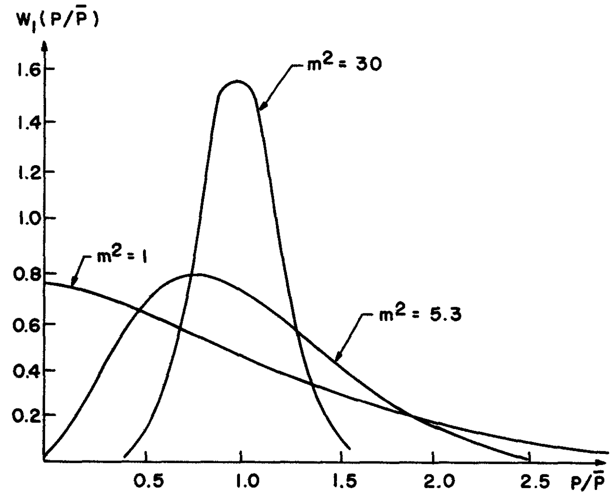

The nature of $f(m^2)$ is such as to suggest that, in a large percentage of the possible $W_1(P/\bar{P})$ cases, identifying and resolving each of two strong targets in ground clutter is definitely possible. Since the most likely, and therefore most prominent, traces on an "A" scope will be those caused by returns that have been reinforced and those that have been cancelled, a comparison of the difference channel "A" scope presentation with the sum channel "A" scope presentation should enable an operator to identify and measure the range of each target.[4]

APPENDIX 2

Comparison Of The Tape Recording With The Filter Output

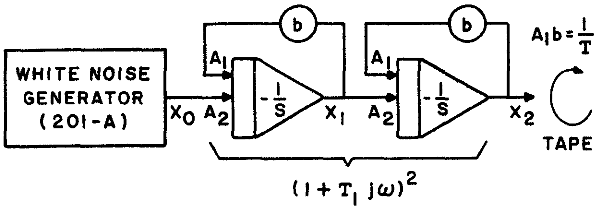

Let $\phi_{xx0}(\tau) = 2T_1\ \delta(\tau)$

1. If $H(j\omega) = (1 + j\,T_1\omega)^{-1}$

then $\phi_{xx1}(\tau) = e^{-|\tau|/T_1}$

where $G_{xx1}(\omega) = \dfrac{2T_1}{1 + T_1^2\omega^2}$

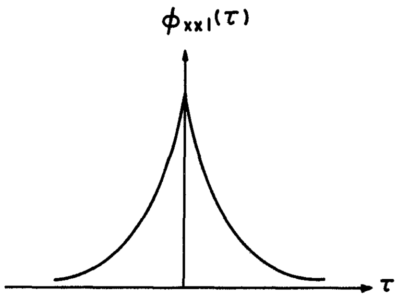

2. Hence

$$\phi_{xx2}(\tau) = \frac{1}{2T_1} \int_{-\infty}^{\infty} \phi_{xx1}(t_1)\ \phi_{xx1}(\tau - t_1)dt_1$$

3. Since the autocorrelation function is an even function, it will be necessary only to solve for the case of $\tau \geq 0$ and use the mirror image of the result for $\tau \leq 0$ in establishing the form of $\phi_{xx2}(\tau)$

$$\phi_{xx2}(\tau) = \frac{1}{2T_1}\left\{ \begin{array}{l} \displaystyle\int_{-\infty}^{0} e^{-\frac{2t_1-\tau}{T_1}} u(-5_1)u(-t_1+\tau)dt_1 \\ \displaystyle+\int_{0}^{\tau} e^{-\tau/T_1} u(t_1)u(-t_1+\tau)dt_1 \\ \displaystyle+\int_{\tau}^{\infty} e^{-\frac{2t_1+\tau}{T_1}} u(t_1)u(t_1-\tau)dt_1 \end{array} \right\} \tau \geq 0$$

4. So,

$$\phi_{xx2}(\tau) = \frac{e^{-\tau/T_1}(|\tau| + T_1)}{2T_1}$$

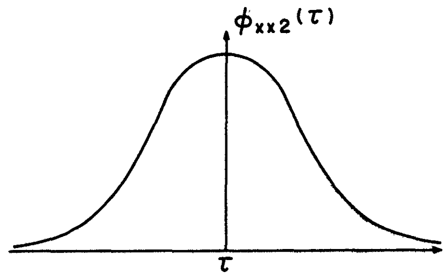

5. It has been shown[5] that if we define

$$\sigma^2(\tau) = \sum \left\{ \left[\phi_{xx2}(\tau) - V(\tau)\right]^2 \right\}$$

where $V(\tau) = \dfrac{1}{T}\displaystyle\int_0^T x_2(t)x_2(t+\tau)dt$

and T = recording time,

then $\sigma^2(\tau) \leq \displaystyle\int_0^{\infty} [\phi(t)]^2\ dt$

6. Substituting for $\phi(t)$,

$$\sigma^2 \leq \frac{4}{T} \int_0^{\infty} \left[\frac{e^{-t/T_1}(t+T_1)}{2T_1} \right]^2 dt$$

$$\therefore\ \sigma^2 \leq 5/4\left(\frac{T_1}{T}\right)$$

APPENDIX 3

Relationship Between The Noise Generator Output And The Filter Output

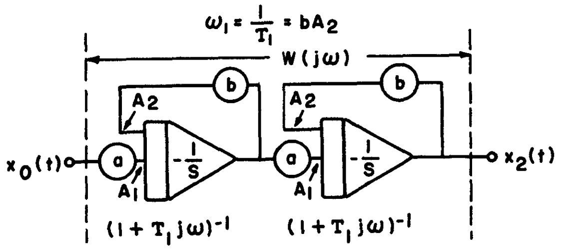

$$W(j\omega) = \frac{aAT_1}{(ST_1+1)} \qquad |W(j\omega)|^2 = \frac{a^2 A_1^2 T_1^2}{(1+T_1^2\omega^2)^2}$$

1. If

$$\Phi(j\omega) \triangleq \frac{1}{2\pi} \int_{-\infty}^{\infty} e^{-j\omega\tau}\, \phi(\tau)d\tau$$

$$\phi(\tau) = \frac{1}{j} \int_{-j\infty}^{j\infty} e^{j\omega\tau}\, \Phi(j\omega)d(j\omega)$$

2. Then

$$\phi_{xx2}(0) = \int_{-\infty}^{\infty} \Phi_{xx2}(j\omega)d\omega$$

or

$$\overline{x_2^2} = \phi_{xx2}(0) = \int_{-\infty}^{\infty} \left|W(j\omega)\right|^2 \Phi_{xx0}(j\omega)d\omega$$

3.

$$\overline{x_2^2} = \frac{a^2 N_0 A_1^2 T^2}{2\pi} \int_{-0}^{\omega_0} \frac{d\omega}{(1+T_1^2\omega^2)^2}$$

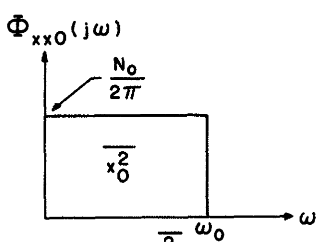

$$\eta_0 = \frac{2\pi \overline{x_0^2}}{\omega_0}$$

4.

$$\therefore \boxed{\overline{x_2^2} = \frac{a^2A^2}{\omega_1^2 2}\left[\frac{1}{1+(\omega_0/\omega_1)^2} + \frac{\omega_1}{\omega_0}\tan^{-1}\frac{\omega_0}{\omega_1}\right]\overline{x_0^2}}$$

$$\overline{x_2^2} = \frac{a_1^2A^2}{2}\left[\frac{1}{\omega_1^2+\omega_0^2} + \frac{1}{\omega_1\omega_0}\tan^{-1}\frac{\omega_0}{\omega_1}\right]\overline{x_0^2}$$

if $\omega_0 \ll \omega_1$

5.

$$\boxed{\overline{x_2^2} \approx \frac{a_1^2A^2}{2}\left[\frac{1}{\omega_0^2} + \frac{1}{\omega_1\omega_0}\frac{\pi}{2}\right]\overline{x_0^2}}$$

REFERENCES

1. Kerr, Propagation of Short Radio Waves, Radiation Laboratory Series, Vol. 13, pp. 550-588, McGraw-Hill, 1951.

2. Lawson and Uhlenbeck, Threshold Signals, Radiation Laboratory Series, Vol. 24, McGraw-Hill, 1947.

3. Bendat, Principles and Applications of Random Noise Theory, John Wiley and Sons, 1958.

4. Shapiro, S.S. Hughes, Improvement of Angular Resolution by Means of Interpulse Frequency Modulation, AFCRC - TN - 59 - 754, on Contract No. AF 19(604)-2625, 15 June 1959.

5. Lanning and Battin, Random Processes in Automatic Control, McGraw-Hill.